

A simple method to obtain ZnO thin films with a hybrid structure of nanoplates and nanorods

LINHUA XU^{1,*}, FENGLIN XIAN¹, JING SU^{1,2}, WENJIAN KUANG¹, MIN LAI^{2,*}

¹*School of Physics and Optoelectronic Engineering, Nanjing University of Information Science & Technology, Nanjing 210044, China*

²*Jiangsu Key Laboratory for Optoelectronic Detection of Atmosphere and Ocean, Nanjing University of Information Science & Technology, Nanjing 210044, China*

In this paper, we reported a simple method to grow Zinc oxide thin films with a hybrid structure of nanoplates and nanorods. As far as we know, no other researchers have obtained ZnO films with this special morphology by sol-gel method. Both X-ray diffraction and photoluminescence indicate that these films have good crystalline quality. In order to test the photocatalytic performance of the samples, a common organic dye, methylene blue (MB), was selected as the photodegradation target. Compared to ZnO films with tightly packed grains and smooth surfaces, the one with a hybrid structure of nanoplates and nanorods exhibits higher photocatalytic efficiency. It is attributed to its higher surface area and easier migration of holes and electrons excited by light to the surface of ZnO nanoplates and nanorods to participate in redox reactions.

(Received August 13, 2024; accepted April 15, 2025)

Keywords: Nanoplate-nanorod hybrid structure, ZnO films, Sol-gel method, Methylene blue, Photocatalytic activity

1. Introduction

Photocatalysis is a green and environment-friendly technique that has currently attracted widespread attention [1-3]. It can be used in the treatment of organic wastewater, reduction of multivalent metal cations, decomposition of water to produce hydrogen gas, antibacterial agent and other fields. Among numerous semiconductors, ZnO is one of the most studied photocatalytic materials. Compared with the photocatalysts in powder form, the photocatalysts in film form is easy to recover and more convenient to use, but their specific surface area is small, which leads to low photocatalytic efficiency. So, lots of researchers are working on how to improve the photocatalytic performance of ZnO films. For example, Daher et al. [4] prepared porous ZnO thin films through dip-coating process, and obtained wrinkled surface morphology by optimizing deposition parameters. The ZnO thin films with wrinkled surface morphology showed better photocatalytic performance. Koji Abe [5] deposited ZnO films with a wrinkle pattern by spin-coating sol approach and found that their photocatalytic performance can be improved by electrochemical reduction. Depth et al. [6] observed that ZnO thin films presented higher photocatalytic performance by forming a heterojunction with silver phosphate (Ag_3PO_4). Segura-Zavala et al. [7] found that modifying the surface of ZnO films with Au-Pd particles can greatly improve their photocatalytic performance. Peter et al. [8] observed that the Cu incorporation in ZnO films can suppress the recombination of electrons and holes and improve visible light absorption, thus leading to an increase in photocatalytic activity. Obviously, it is one

of the simplest and most ideal ways to improve the photocatalytic efficiency of ZnO films by tailoring their morphology. In this study, we found that co-doping of Al and Na into ZnO thin films can lead to the formation of a hybrid structure of nanorods and nanoplates. This special structure exhibits good crystal quality and high photocatalytic efficiency. By consulting literatures, it can be known that there are currently no relevant reports on the hybrid structure of nanorods and nanoplates produced by sol-gel process.

2. Experimental

In order to obtain ZnO films, the precursor solutions were first prepared. $\text{Zn}(\text{CH}_3\text{COO})_2 \cdot 2\text{H}_2\text{O}$ was the zinc source; $\text{C}_2\text{H}_5\text{OH}$ was solvent. $\text{C}_2\text{H}_7\text{NO}$ was a chelating agent. $\text{AlCl}_3 \cdot 6\text{H}_2\text{O}$ and NaCl were used as doping sources. Relative to zinc, the doping concentration of aluminum is 8at. % and that of sodium is 6 at. %. The precursor solution was dropped onto the Si substrate with a size $2.0 \text{ cm} \times 2.0 \text{ cm}$ and then spread to form a gel film by rotating the substrate; and then the thin film was pre-heated at $300 \text{ }^\circ\text{C}$ for 3 minutes. Spin-coating and preheating were repeated 8 times. Pure, Al-doped, Na-doped, and Al-Na co-doped ZnO films were prepared. These samples were post-annealed at $450 \text{ }^\circ\text{C}$ for one hour to obtain the crystallized films.

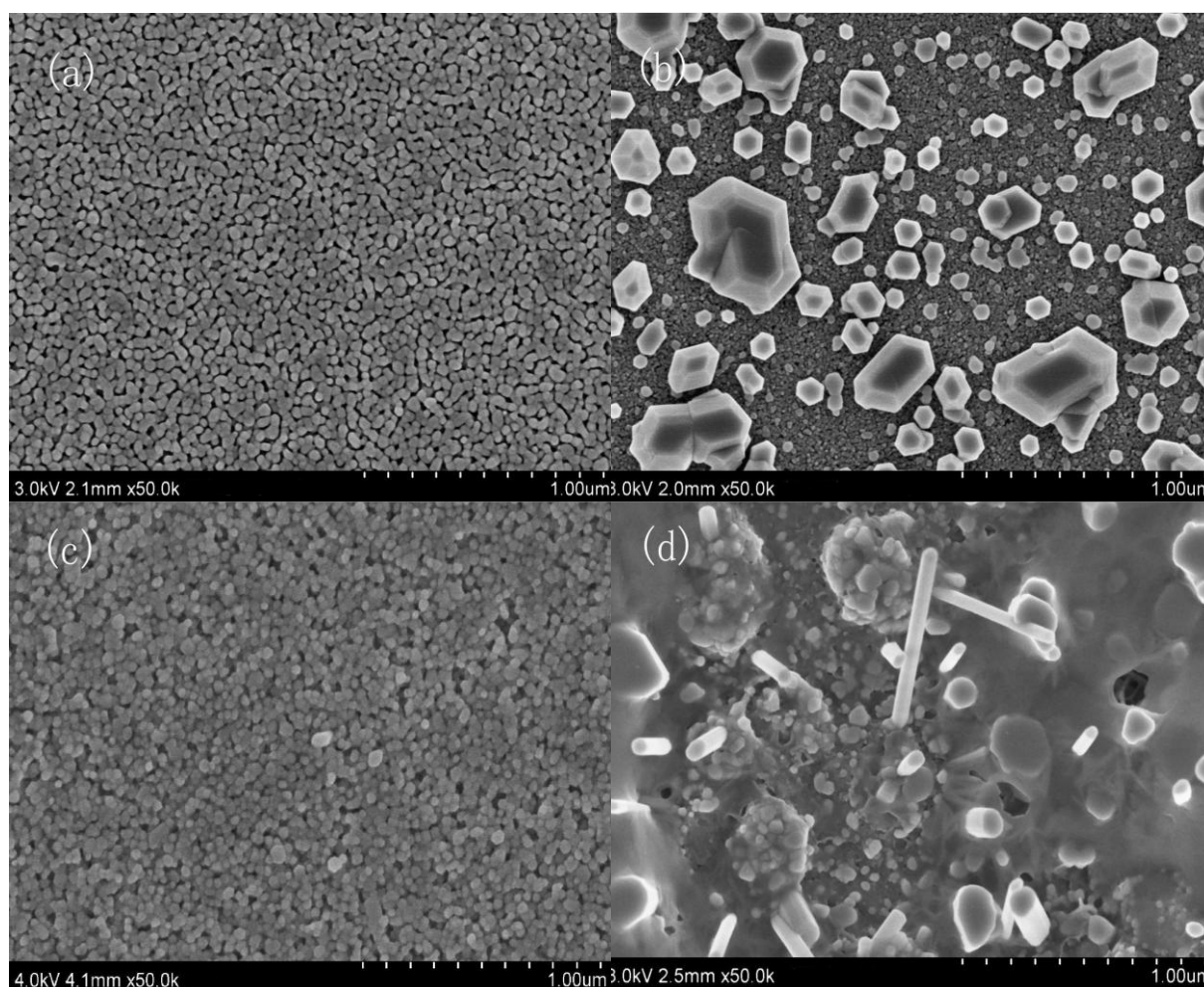
Bruker D8 diffractometer was utilized to determine the crystalline state of the samples. SEM images were adopted to reveal the morphology of the films by S4800 microscope. The composition and distribution of doped elements were decided by XPS and EDX spectra. The

photoluminescence spectra were recorded by LabRAM HR800. The absorbance of MB was measured by a UV-VIS spectrophotometer (TU-1901).

3. Results and discussion

Fig. 1 exhibits the morphology of the samples. For the pure ZnO film, its grains are very uniform, with an average particle size of about 50 nm. After doping with aluminum, some pyramid-like nanostructures appeared on the ZnO film surface. Previous studies have shown that the pyramid-shaped particles have high crystal quality and exhibit the characteristic of single crystals. [9]. After sodium is doped into the ZnO film, the grains slightly decrease and several nanorods appear. This morphological change is similar to the results observed by Fan et al. [10]. When Al and Na are co-doped into ZnO thin films, a mixed structure of nanorods and nanoplates appears on the film surface. The diameter of these nanorods is very uneven, ranging from 20 to 200 nm. The length of the

nanorods varies from 200 to 1000 nm. From Fig. 1 (f), it is able to be confirmed that the thickness of the nanoplates ranges from 20 to 50 nm. The emergence of nanoplates and nanorods has greatly increased the number of active sites and the probability of photogenerated charge carriers participating in redox reactions on the surface. The evolution of this morphology is related to the doping of sodium and more chloride. Since both sodium chloride [10] and aluminum chloride [11, 12] as individual dopants can cause the appearance of nanorods on the surface of ZnO thin films, while aluminum nitrate [13] as a dopant cannot induce the appearance of nanorods, the doped chloride ions should be the main factor causing the appearance of nanorods. When sodium chloride and aluminum chloride are co-doped into ZnO thin films, the incorporation of sodium ions and more chloride ions will cause significant changes in the surface energy of ZnO thin films, resulting in the coexistence of nanorods and nanoplates. The specific growth mechanism is still under further study.



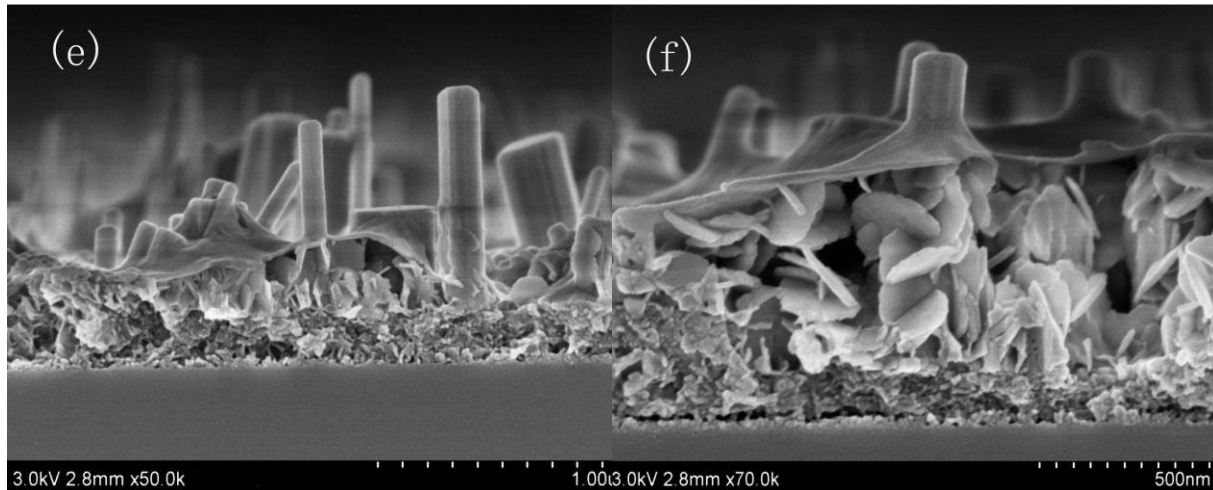


Fig. 1. SEM images of pure (a), Al-doped (b), Na-doped (c) and Al-Na co-doped (d, e, f) ZnO thin films

Fig. 2 gives the XRD spectra of the films. All samples exhibit strong (002) diffraction peaks, indicating that grains in the ZnO films are preferentially oriented along the c-axis direction. Compared with the pure ZnO film, Na-doping slightly reduces the intensity and increases the half maximum width of the (002) diffraction peak, indicating a decrease in grain size, which is consistent with the results observed from SEM images. However, the (002) peak of the ZnO film co-doped with Al and Na is greatly enhanced, indicating that the c-axis orientation of the film is improved.

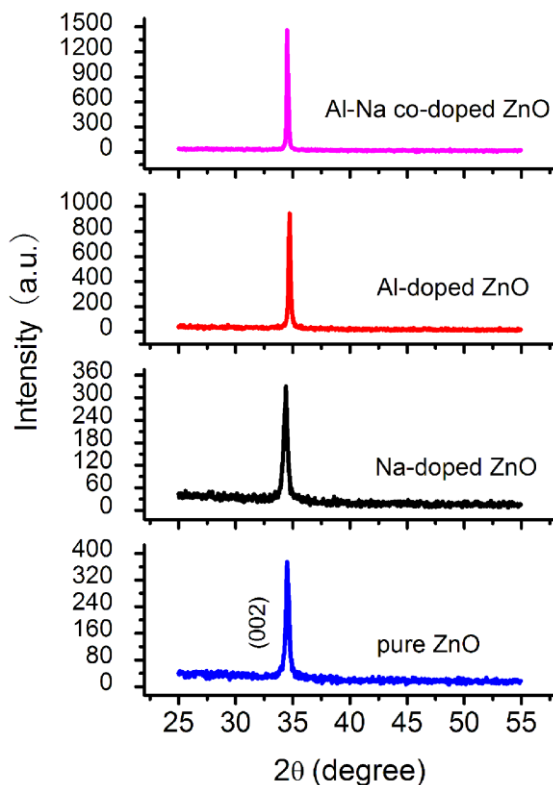


Fig. 2. XRD patterns of the samples (colour online)

The XPS spectra of the film co-doped with Al and Na are displayed in Fig. 3. From the survey scan spectrum in Fig. 3 (a), no signals from other substances are observed except for zinc and oxygen, as well as intentionally doped Na, Al, and Cl. Fig. 3 (b) shows that the high-resolution O 1s XPS spectral line which is not geometrically symmetric, meaning the presence of different oxygen-containing species. Gaussian fitting is performed on it, and the fitting result shows the presence of two sub-peaks. One sub-peak is located at 530.6 eV; it comes from the lattice oxygen bound to Zn [9]. The other sub-peak is located at 532.3 eV, and this signal may come from two sources. One is the oxygen-containing substances on the sample surface, such as physically adsorbed oxygen or hydroxyl groups. Another is lattice oxygen bound to Al ions [14]. Fig. 3 (c) shows the two peaks of Zn 2p_{3/2} and Zn 2p_{1/2}. From the position of the peaks and the energy difference between them, it is suggested that Zn has already been oxidized to Zn²⁺ [9]. Fig. 3 (d-f) displays the XPS signal peaks of Al, Cl, and Na, indicating that these elements have been doped into ZnO lattices and exist in +3, -1 and +1 valence states, respectively.

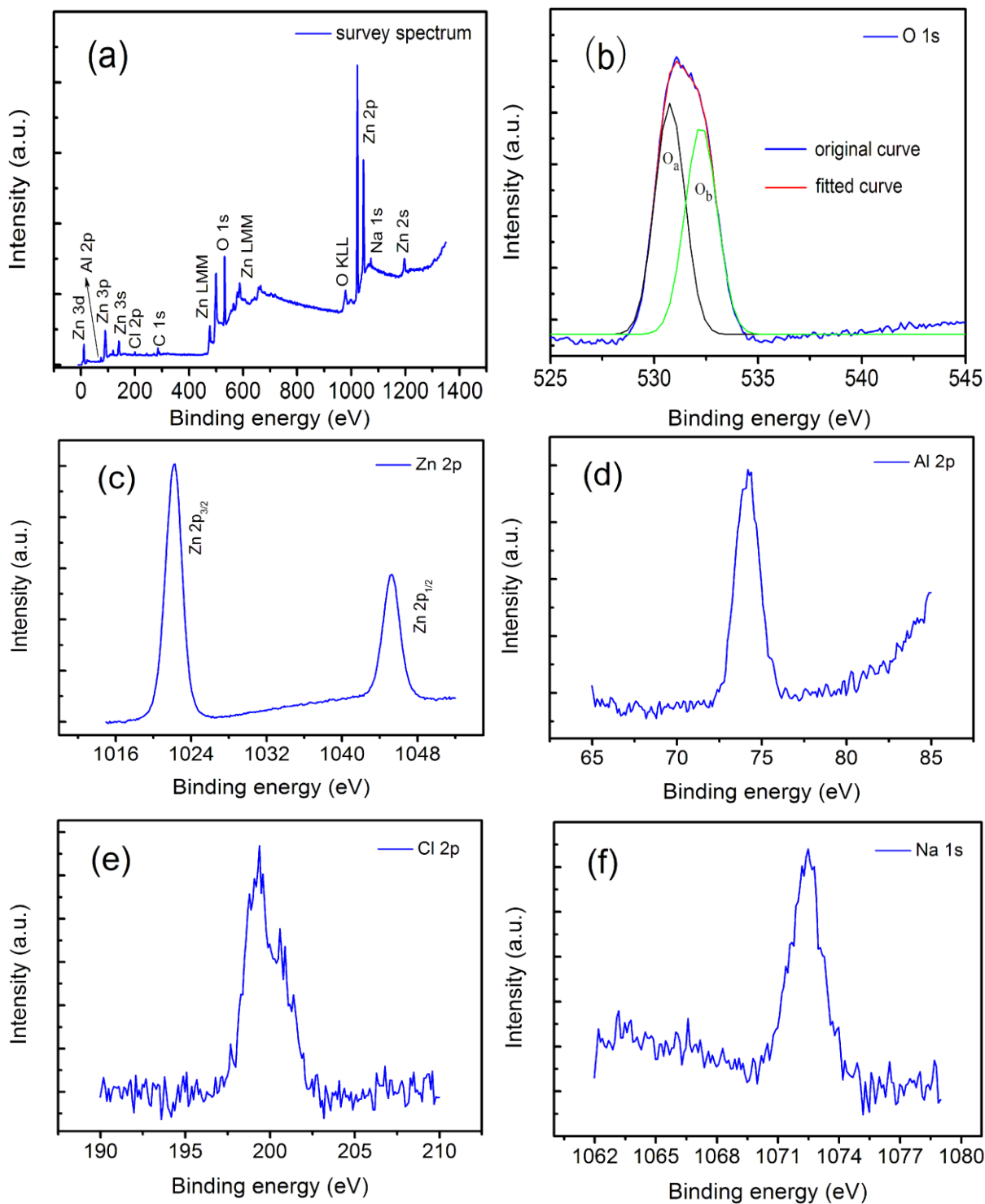


Fig. 3 XPS spectra of Al-Na co-doped ZnO thin film: (a) survey scan, (b) O 1s, (c) Zn 2p, (d) Al 2p, (e) Cl 2p and (f) Na 1s (colour online)

In order to more know the distribution of Al, Cl, and Na, we tested EDX spectra at different positions of Al-Na co-doped ZnO films, as shown in Fig. 4.

It can be observed that no Na signal was detected in the nanorod, but Na signal was detected in the underlying film. This means that the distribution of Na in the sample is nonuniform.

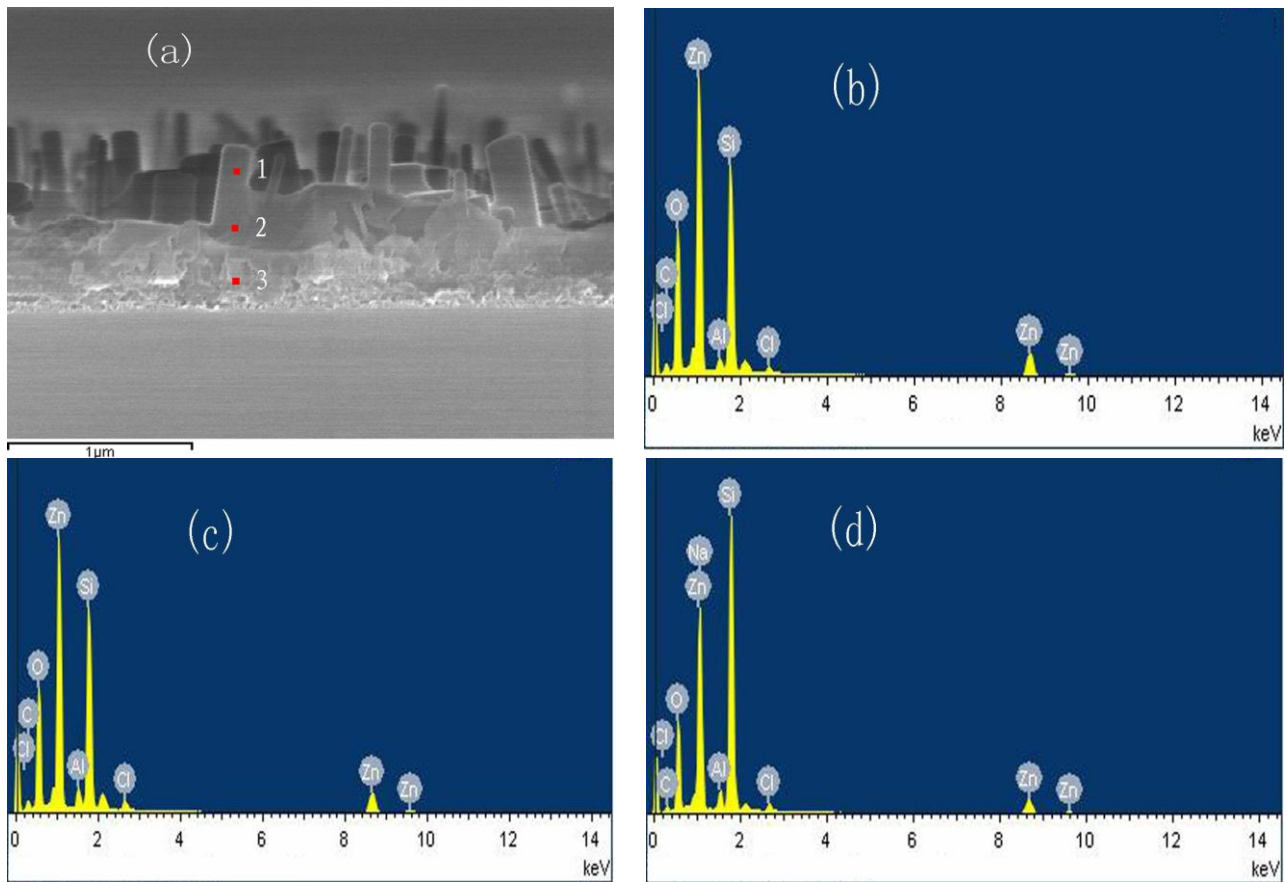


Fig. 4. EDX spectra at different positions of the Al-Na co-doped thin film (colour online)

Fig. 5 exhibits the PL spectra. The 380 nm emission is the intrinsic emission of ZnO, which is generated by free exciton recombination. This UV emission is very sensitive to the crystalline quality. When ZnO has better crystalline quality, it will produce the higher UV emission efficiency [15]. When Na is doped alone, the UV emission slightly decreases because of a slight decline in the crystalline quality of ZnO. However, when Al is doped alone or Al-Na is co-doped, the UV emission is greatly increased, which is attributed to the highly crystalline nanorods and nanosheets grown on the ZnO film surface. The case above is similar to the results reported by Fan et al. [10]. For the very weak red emission centered at 650 nm, although its emission mechanism is still controversial, some researchers believe that it may be related to the oxygen interstitials or excess oxygen adsorbed on ZnO surface [16]. The PL peak at ~ 760 nm is the secondary UV (380 nm) diffraction [17].

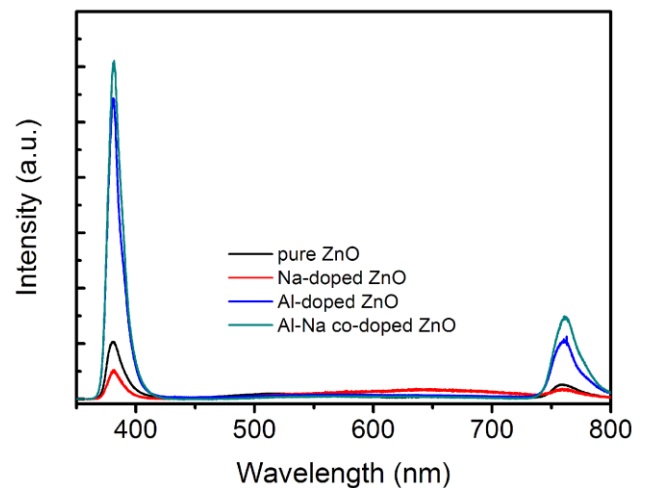


Fig. 5. Photoluminescence spectra of the samples (colour online)

Using the Al-Na co-doped sample as the photocatalyst, the absorbance curves of photodegraded MB solution are plotted in Fig. 6 (a). The initial solution of MB is 5 mg/L. A Xe lamp was used as the light source (simulating the solar spectrum). The absorbance gradually decreases with the photocatalytic reaction time prolonging. This suggests that the MB concentration is gradually reducing. Using the formula presented in [18], the efficiency of photodegradation of methylene blue was calculated. As can be observed from Fig. 6(b), the photocatalytic activity

of the film with a nanosheet-nanorod hybrid structure is greatly improved in contrast to the pure ZnO film. The enhancement of photocatalytic performance is mostly ascribed to two factors: (1) the nanorods and nanosheets possess higher crystalline quality, resulting in generate more electrons and holes under excitation of light; (2) The photoproducted holes and electrons are easier to migrate to the surface of nanorods and nanosheets and participate in redox reactions.

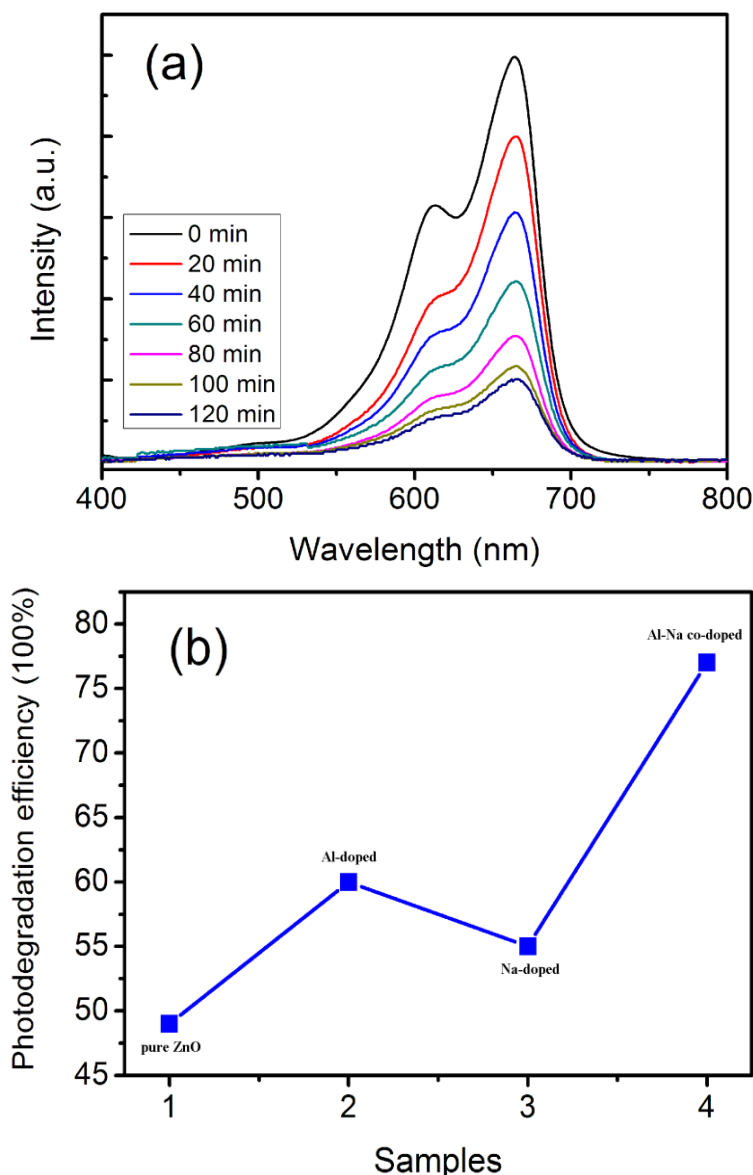


Fig. 6. (a) The absorbance curve of methylene blue and (b) Photodegradation efficiency of different samples (colour online)

4. Conclusions

In this study, we found that the co-doping of AlCl_3 and NaCl led to the appearance of a hybrid structure of nanoplates and nanorods on the surface of ZnO films. In contrast to pure ZnO films with smooth surfaces and dense grains, the ones with a hybrid structure of nanoplates and

nanorods have a higher specific surface area. At the same time, photoproducted holes and electrons have more chance to migrate to the surface of nanoplates or nanorods to react with dye molecules. The better photocatalytic performance of ZnO films with this special morphology has been demonstrated by the experiments of photodegradation of MB. Given the simplicity and low cost of the method for

producing this special morphology film, it has potential applications in future organic wastewater treatment.

Acknowledgements

Professor Min Lai thanks the financial support by the National Natural Science Foundation of China (Grant no. 62275126).

References

- [1] Y. Song, J. Liu, X. Wang, H. Liang, J. Bai, *Optical Materials* **148**, 114825 (2024).
- [2] Z. Yousefzadeh, M. Montazer, A. Mianehro, *Carbohydrate Polymers* **326**, 121622 (2024).
- [3] Y. Wu, T. V. Tam, P. Rao, W. M. Choi, I.-K. Yoo, *Applied Surface Science* **654**, 159490 (2024).
- [4] E. A. Daher, B. Riachi, J. Chamoun, C. Laberty-Robert, W. Hamd, *Colloids and Surfaces A: Physicochemical and Engineering Aspects* **658**, 130628 (2023).
- [5] K. Abe, *Int. J. Electrochem. Sci.* **16**, 21106 (2021).
- [6] V. Deepthi, B. Vidhya, A. Sebastian, *Optical Materials* **138**, 113646 (2023).
- [7] J. Segura-Zavala, O. Depablos-Rivera, T. García-Fernandez, M. Bizarro, R. E. García-Morales, C. Sanchez-Ake, *Thin Solid Films* **776**, 139884 (2023).
- [8] R. Peter, A. Omerzu, I. Kavre Piltaver, R. Speranza, K. Salamon, M. Podlogar, K. Velican, M. Percic, M. Petravic, *Ceramics International* **49**, 35229 (2023).
- [9] L. Xu, X. Wang, F. Xian, J. Su, *Materials Research Bulletin* **123**, 110724 (2020).
- [10] H. Fan, Z. Yao, C. Xu, X. Wang, Z. Yu, *Journal of Electronic Materials* **47**, 3847 (2018).
- [11] N. Huang, C. Sun, M. Zhu, B. Zhang, J. Gong, X. Jiang, *Nanotechnology* **22**, 265612 (2011).
- [12] L. Xu, F. Xian, S. Pei, Y. Zhu, *Optik* **203**, 164036 (2020).
- [13] A. Zang, K. Chen, L. Xu, F. Xian, W. Ma, Z. Tian, *Current Applied Physics* **54**, 59 (2023).
- [14] V. Chauhan, R. Kumar, *Superlattices and Microstructures* **141**, 106389 (2020).
- [15] A. Al-Nafiey, B. Sieber, B. Gelloz, A. Addad, M. Moreau, J. Barjon, M. Girleanu, O. Ersen, R. Boukherroub, *J. Phys. Chem. C* **120**, 4571 (2016).
- [16] T. Chen, G. Z. Xing, Z. Zhang, H. Y. Chen, T. Wu, *Nanotechnology* **19**, 435711 (2008).
- [17] N. Han, P. Hu, A. Zuo, D. Zhang, Y. Tian, Y. Chen, *Sensors and Actuators B* **145**, 114 (2010).
- [18] X. Zhang, J. Qin, R. Hao, L. Wang, X. Shen, R. C. Yu, S. Limpanart, M. Z. Ma, R. Liu, *J. Phys. Chem. C* **119**, 20544 (2015).

*Corresponding author: congyu3256@sina.com;
mlai@nuist.edu.cn